PAPER

Tb³⁺–atorvastatin doped in poly(ethylene glycol) optical biosensor for selective determination of progesterone and testosterone in serum samples

Mohamed S. Attia,*[a] Safwat A. Mahmoud, [iD] [b] Amal M. Ahmed,[a] Tarek A. Amin,[a] Ahmed. O. Youssef,[a] Mohammed A. Amin, [iD] [c] Mona N. Abou-Omar[d] and Ekram H. Mohamed [iD] *[e]

An innovative, simple and cost effective Tb³⁺–atorvastatin photo probe was designed and used as a core for a spectrofluorometric approach to sensitively determine two vital biological compounds in serum samples. Tb³⁺–atorvastatin complex displays a characteristic electrical band with λ_{em} at 545 nm with significant luminescence intensity, which is quenched in the presence of progesterone and testosterone at two variant sets of pH; 6.2 and 7.5, respectively. The conditions were optimized and the best solvent for operation was found to be acetonitrile with λ_{ex} at 320 nm. Progesterone and testosterone were assessed in serum samples using the same optimal conditions within concentration ranges of 2×10^{-9} to 2.9×10^{-6} and 3.1×10^{-9} to 4.8×10^{-6} mol L^{-1}, respectively. The proposed luminescence method was validated in accordance to ICH guidelines and found to be accurate, precise and specific and free from any interference. The cost effectiveness and applicability of the method make it a good choice for routine analysis of the two compounds and early diagnosis of chronic diseases associated with abnormalities in their physiological levels.

1. Introduction

Progesterone (PGS) is a member of the progestogen steroid hormones group, secreted mainly during the menstrual cycle by the corpus luteum preparing the body for conception in case of ova fertilization.[1] PGS is used in oral contraception either in single form or combined with estrogen and as hormonal replacement therapy to alleviate menopause symptoms. Low levels of progesterone may lead to abnormal bleeding during menstruation, premature labor and miscarriage during pregnancy and is considered a sign for poly-cystic ovarian syndrome. Elevated PGS levels may increase the risk of breast cancer development and are a marker for adrenal hyperplasia. PGS concentration was recently estimated using different analytical approaches; spectroscopic,[2] chromatographic,[3,4] and electrochemical methods[5,6] and immunological assay[7,8]

Testosterone (TST), an anabolic steroid, is the primary male sex hormone where it regulates RBCs production, libido, fertility, spermatogenesis, fat distribution, bone and muscle mass.[9,10] Imbalance in levels of TST may can cause serious body dysfunctions where diminished levels have an inverse impact on sexual drive, erection, sperm count and muscle strength. Abnormally high TST levels may trigger early puberty in males and menstrual irregularities and baldness in females.[11,12] TST could also be used as a medication to replenish its insufficiency, manage breast cancer in women and enhance physique and performance, for instance in athletes.[13,14] Its concentration in different matrices such as plasma, serum, and saliva was recently measured through spectroscopic[15,16] chromatographic[9,11,17] and electrochemical methods[18] and capillary electrophoresis.[19] Fig. 1 displays the structure of PGS and TST.

The reported methods showed relatively high limits of detection which restricts their practical applications. Moreover, the measurement of low concentrations of, progesterone and testosterone in biological samples along with interference from some biomolecules such as uric acid (UA), ascorbic acid (AA), and different hormones requires to efficiently improve the sensitivity of chromatographic methods and the electrochemical sensors for practical applications. Therefore, developing a simple method for accurate determination of progesterone and testosterone in the presence of each other in

[a]*Chemistry Department, Faculty of Science, Ain Shams University, Cairo 11566, Egypt. E-mail: Mohd_mostafa@sci.asu.edu.eg; Mohamed_sam@yahoo.com; Tel: +202 1229867311; +202 1060819022*

[b]*Physics Department, Faculty of Science, Northern Border University, Arar, Saudi Arabia*

[c]*Department of Chemistry, Collage of Science, Taif University, P. O. Box 11099, Taif 21944, Saudi Arabia*

[d]*Department of Chemistry, Faculty of Women for Arts, Science and Education, Ain Shams University, Cairo, Egypt*

[e]*Pharmaceutical Analytical, Chemistry Department, Faculty of Pharmacy, The British University in Egypt, El Sherouk City, Cairo, 11837, Egypt. E-mail: ekram.hany@bue.edu.eg*
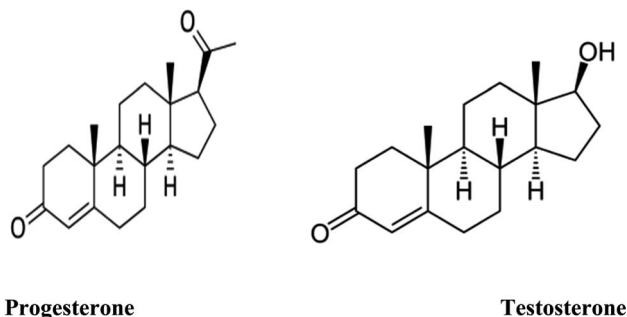
Progesterone   **Testosterone**

Fig. 1 Chemical structure of progesterone and testosterone.

the same sample is still of great significance. Today, the research field in which the lanthanide complexes were used as biosensors has a great interest.[20–30] Luminescent optical biosensor Tb (atorvastatin)$_3$ (Tb–Ator) complex embedded in PEG matrix have many advantages over the mentioned traditional methods. The chemical structure of atorvastatin is presented in Fig. 2. Terbium ion has sharp and precise emission bands in green light region. The terbium ion is used as photo probe for many analytes with a high selectivity depends on the excitation wavelength of terbium–analyte complex, pH and the type of solvent of the test solution. Doping of the optical sensors in the polymer matrix increases its stability and durability.[24–30] The sensor can provide a constant signal response for two years, which makes it 24-fold better balance compared to the lifetime warranted for the chromatographic and electrochemical methods. The source of error of the present work eliminated as it more stables for a long time; it gives a low standard deviation value. The higher stability of the current sensor can be attributed to the doping of the optical sensor in the polymer matrix.

2. Experimental

2.1. Instrumentation

A double beam UV-Visible spectrophotometer (PerkinElmer Lambda 25), fluorescence Spectrometer (Thermo Scientific Lumina, Meslo-PN; 222-263000). pH meter (Jenway; 33300).

2.2. Materials and reagents

Progesterone and testosterone, solvents including ethanol, acetonitrile, dimethylformamide (DMF), chloroform and dimethyl sulfoxide (DMSO) were purchased from Sigma Aldrich. Analytical grade ammonium hydroxide (NH$_4$OH), hydrochloric
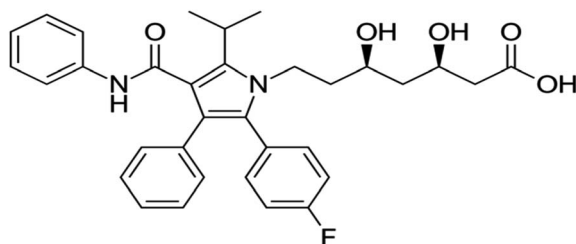

Fig. 2 Chemical structure of atorvastatin.

acid (HCl), Tb (NO$_3$)$_3$·5H$_2$O, atorvastatin and polyethylene glycol (PEG) were purchased from Sigma Aldrich.

The human real samples were gathered from both Ain Shams Specialized and Teaching New Al-Kasr-El-Aini Hospitals, Cairo, Egypt in accordance with the approved protocol of World Health Organization (WHO) for the collection of human specimens and the use of the clinically related information and data for the purpose of research. The patients approved and were all consented before using their samples.

2.3. Preparation of standard solutions

Stock solutions of Tb (NO$_3$)$_3$·5H$_2$O and atorvastatin; were prepared separately by accurately weighing and transferring 0.11 g and 0.039 g, respectively of their authentic pure forms into separate 25 mL volumetric flasks by the aid of the least amount of ethanol till dissolution and completing the volume with the same solvent to obtain final concentration of (10^{-2} mol L^{-1}) for each of them.

Tb^{3+}–atorvastatin complex solution; was prepared by mixing 0.1 mL of Tb (NO$_3$)$_3$ stock solution with 0.3 mL of atorvastatin stock solution in 10 mL volumetric flask and completing the volume to the mark with acetonitrile.

For the two compounds under study, all stock solutions were separately prepared in 10 mL volumetric flasks in concentration of solution (10^{-2} mol L^{-1}). This was achieved by dissolving for PGS and TST 0.031 g and 0.0288 g were dissolved, respectively in small amount of ethanol and then volume was diluted to the mark with acetonitrile. Further dilutions for the stock solutions using acetonitrile were performed to obtain working solutions with concentrations of 1.0×10^{-4} to 1.0×10^{-9} mol L^{-1} of PGS and TST.

0.1 mol L^{-1} of NH$_4$OH and HCl were used to adjust the pH to 6.2, 7.5 for PGS and TST, respectively. All the prepared solutions should be kept at low temperature (2–8 °C) to remain stable.

2.4. Preparation serum samples spiked with PGS and TST

A 1.0 mL of samples of blood collected from healthy volunteers was centrifuged for 15 min at 4000 rpm to remove proteins. 0.1 mL of the serum sample was added to 1.0 mL of each drug
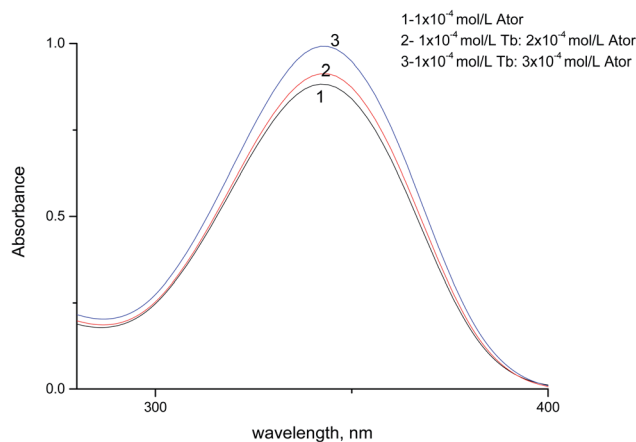

Fig. 3 The absorption spectra of (1) atorvastatin (1.0×10^{-4} mol L^{-1}), (2) 2.0×10^{-4} mol L^{-1} atorvastatin: Tb^{3+} (1.0×10^{-4}), (3) 3.0×10^{-4} mol L^{-1} atorvastatin: Tb^{3+} (1.0×10^{-4} mol L^{-1}).
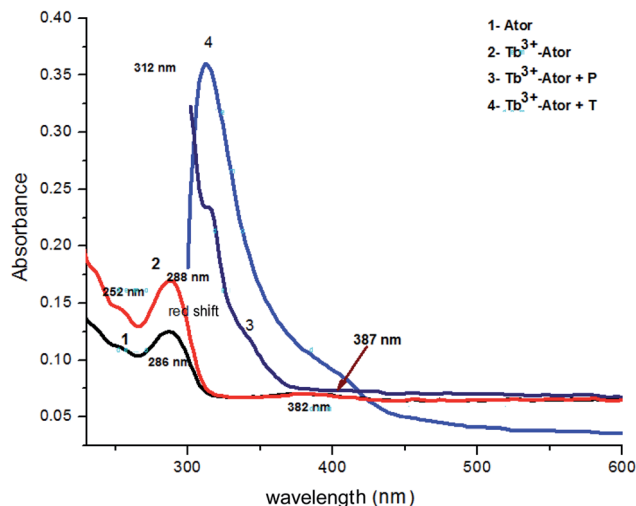
Fig. 4 The absorption spectrum of (1) atorvastatin, (2) Tb^{3+}−atorvastatin complex (Tb^{3+}−Ator), (3) Tb^{3+}−atorvastatin complex (Tb^{3+}−Ator)−progesterone (P), (4) Tb^{3+}−atorvastatin complex (Tb^{3+}−Ator)−testosterone (T).

working solution of concentration 1.0×10^{-6} mol L^{-1} and the volume was complete to 10 mL by acetonitrile to obtain 1.0×10^{-7} mol L^{-1} for each drug in four separate 10 mL measuring flasks.

2.5. Preparation of Tb–Ator biosensor embedded in PEG

Tb–Ator complex was prepared in the solid state by mixing an equal volume of 1.0×10^{-4} mol L^{-1} Tb ion and 3.0×10^{-4} mol L^{-1} atorvastatin in ethanol, then evaporation near the dryness of the solution, a pale pink solid was obtained after cooling in air. The thin film was prepared by dissolving 0.1 g of the solidified and seamless complex in 3 mL ethanol and then adding 10 mL of viscose freshly prepared PEG with stirring for about one hour until a homogenous solution was obtained. A thin film was fabricated by spin-coating on a small quartz slide
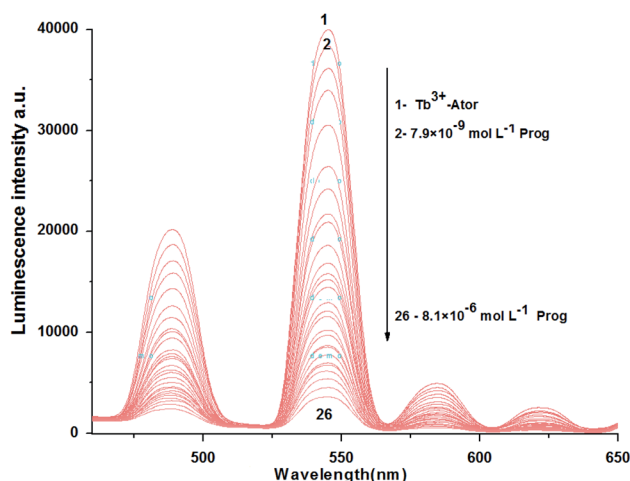

Fig. 5 The emission spectra of Tb^{3+}−Ator complex at $\lambda_{ex} = 320$ nm and pH 6.2 in presence of different progesterone concentrations using acetonitrile as a solvent.

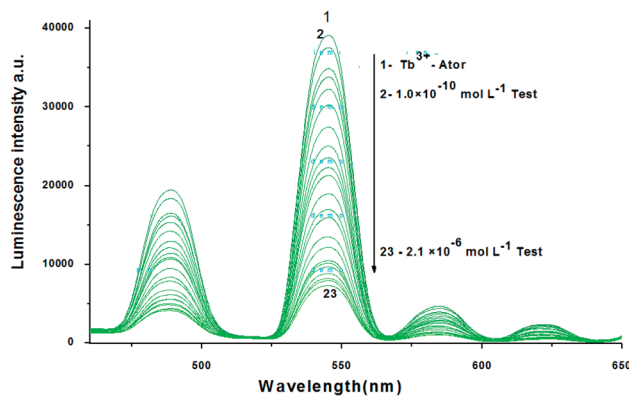Fig. 6 The emission spectra of Tb^{3+}−Ator complex at $\lambda_{ex} = 320$ nm and pH 7.5 in presence of different testosterone concentrations using acetonitrile as a solvent.

(width 8.5 mm, height 25 mm) to quick fit in the cuvette of the spectrofluorometer.

2.6. Recommended procedure

An appropriate volume (100 μL) of various standard concentrations of progesterone and testosterone should be diluted to 3 mL with acetonitrile. The dilute solution was mixed with a thin film of biosensing Tb–Ator doped in PEG matrix in the quartz cell of a spectrofluorometer. The luminescence spectra were recorded at the excitation wavelength $\lambda_{ex} = 320$ nm. After each measurement, the optical sensor was washed with acetonitrile, and the calibration curve was built by applying the Stern's Volmer equation by plotting (F/F_0) the at $\lambda_{em} = 545$ nm on the y-axis versus the progesterone and testosterone concentration in mol L^{-1} on the x-axis.

2.7. Determination of progesterone and testosterone in serum samples

The luminescence spectra of the serum samples previously prepared as described under (2.4) were measured adopting the same procedures followed under (3.2). The concentrations of each real sample were calculated using corresponding regression equation.

3. Result and discussion

3.1. General features of absorption and emission spectra of Tb–Ator complex

Owing to the f–f transition forbiddance of trivalent ion (Tb^{3+}), there is a restriction to directly absorb light which could be overcome through the antenna effect via the coupling between Tb^{3+} and a prominently absorbing organic ligand leading to efficient energy transfer and light absorption processes. Regarding the proposed photo probe, Tb^{3+} is surrounded covalently by 3 molecules of atorvastatin ligand responsible for efficient absorption of light and transfer of energy to populate $^5D_4$ state of Tb^{3+}.[31]

The emission of the formed complex Tb–Ator exhibited four specific and intense bands because of the $^5D_4$–^7F_J transitions (J = 6, 5, 4 and 3).[32–40]
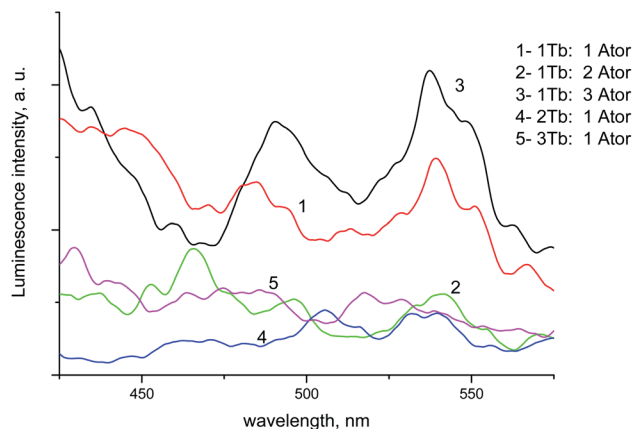
Fig. 7 Luminescence emission spectra of Tb^{3+} with different molar ratio of Ator in acetonitrile at $\lambda_{ex} = 320$ nm and pH 6.8.

3.2. Absorption and emission spectra

The absorption spectra of atorvastatin and Tb^{3+} with different concentrations of atorvastatin are shown in Fig. 3. A red shift by 7 nm and the absorbance value is enhanced denoting that atorvastatin could form a stable complex with Tb^{3+}. The absorption spectra of PGS and TST were scanned in the presence of the optical sensor are shown in Fig. 4.

The emission spectra of Tb^{3+}–atorvastatin complex after adding different concentrations of PGS and TST using acetonitrile as solvent are shown in Fig. 5 and 6, respectively. The characteristic electrical emission band of Tb^{3+} exhibited at λ_{em} 545 nm was quenched due to energy transfer from the optical sensor to PGS and TST.

3.3. Experimental variables

3.3.1 Tb^{3+} and atorvastatin amounts. The Tb^{3+}–atorvastatin complex was formed in ratio 1 M : 3 L indicating that the metal coordinates to the ligand at different sites of coordination not *via* oxygen only, Fig. 7.

3.3.2 Solvent effect. The intensity of luminescence of solutions containing Tb^{3+} (1.0×10^{-4} mol L^{-1}) and atorvastatin

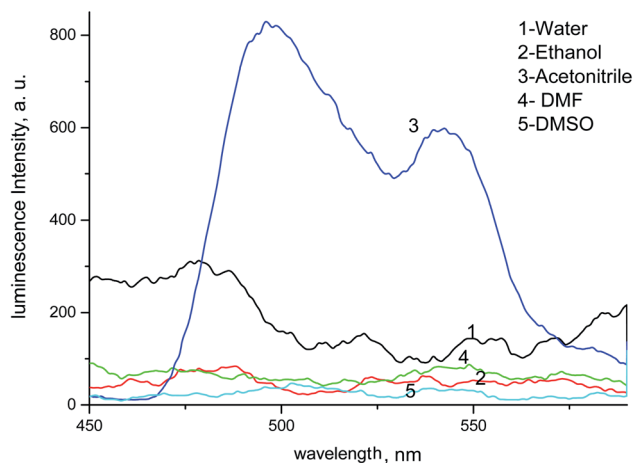$(3.0 \times 10^{-4}$ mol L^{-1}) was investigated in different solvents and the results revealed that maximum enhancement was noticed in acetonitrile as presented in Fig. 8. Solvents with hydroxyl group as ethanol diminishes the luminescence intensity due to transfer of vibrational energy to molecules of solvents.[41–45]

3.3.3 pH effect. The medium pH has a significant influence on the luminescence intensity of the formed Tb^{3+}–atorvastatin complex. Solutions of NH_4OH and HCl, both 0.1 mol L^{-1} were used for pH adjustment. The highest luminescent intensity at λ_{em} 545 nm was observed at pH = 6.8 as shown in Fig. 9.[46–48]

3.3.4 Mechanism of emission quenching. Upon adding different concentrations of PGS and TST to the Tb–Ator photo probe a notified quenching in its luminescent intensity occurs owing to the approach of the analytes under study and formation of H-bond between the hydroxyl group in both of TST and enol group in PGS with the atorvastatin. The formation of H-bonding lead to the depression or decrease in the transfer of energy to the Tb^{3+} ion and consequently the luminescence intensity is significantly quenched.

The pH effect on the luminescence intensity after the addition of the studied analytes to the proposed photoprobe was

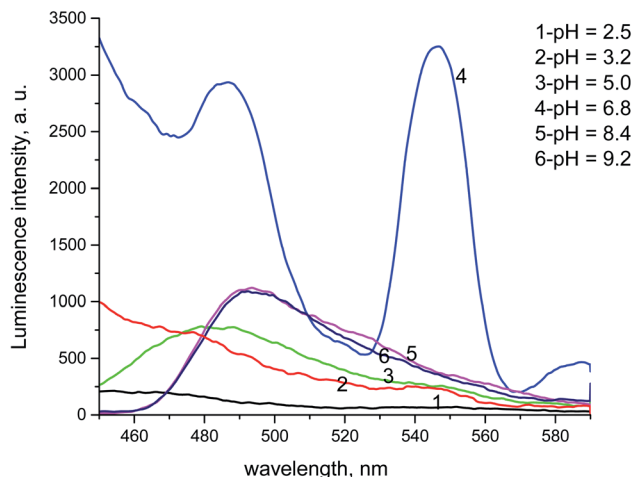**Fig. 9** Emission spectra of Tb^{3+}–Ator optical sensor in acetonitrile at $\lambda_{ex} = 320$ nm and different pHs.

Fig. 8 Emission spectra of Tb^{3+}–Ator optical sensor in different solvents at $\lambda_{ex} = 320$ nm and pH 6.8.
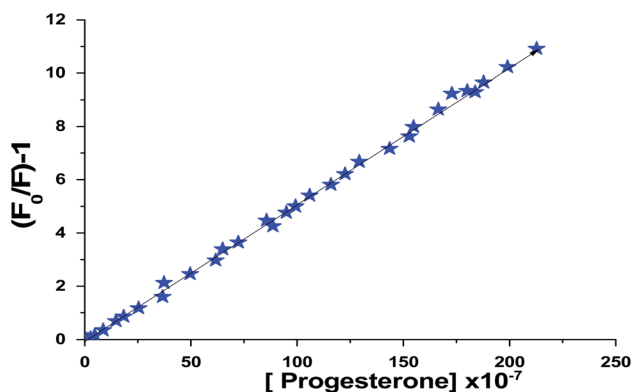

Fig. 10 Stern–Volmer plot $(F_0/F) - 1$ against corresponding concentrations of progesterone.
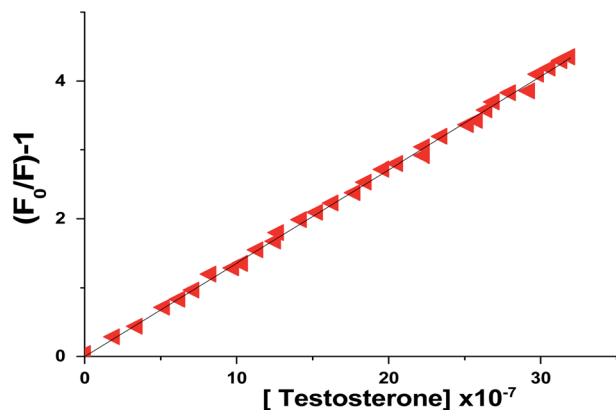
Fig. 11 Stern–Volmer plot $(F_0/F) - 1$ against corresponding concentrations of testosterone.

Table 1 Validation sheet and parameters of the regression equations of the proposed optical sensor

Parameter	Progesterone	Testosterone
λ_{em} (nm)	545	
Linearity (mol L^{-1})	$(2 \times 10^{-9}$ to $2.9 \times 10^{-6})$	$(3.1 \times 10^{-9}$ to $4.8 \times 10^{-6})$
LOD (mol L^{-1})	8.5×10^{-10}	7.02×10^{-10}
LOQ (mol L^{-1})	2.5×10^{-9}	2.1×10^{-9}
Regression equation	$(Y = a + bX)^a$	
Intercept (a)	47.2	105
Slope (b)	3.1	2.2
Standard deviation	15.5	20.5
Variance (S^2)	240.25	420.25
Regression coefficient (r)	0.99	0.99

^{a} Where Y: intensity of luminescence, X: analyte concentration (mol L^{-1}), a: intercept and b: slope.

studied and the luminescence quenching was observed at pH 6.2 and 7.5 for PGS and TST, respectively.

3.4. Analytical performance[49]

3.4.1 Linearity. Correlations between the luminescence of emission intensity of optical sensor at λ_{em} 545 nm and PGS and

TST within concentration ranges of $(2 \times 10^{-9}$ to $2.9 \times 10^{-6})$ and $(3.1 \times 10^{-9}$ to $4.8 \times 10^{-6})$ mol L^{-1} respectively were found to be linear as presented in respective calibration graphs, Fig. 10 and 11 obtained by applying the Stern–Völmer plot.

The Stern–Volmer constant and critical concentration of PGS and TST values are $(\kappa_{sv} = 3.1$ and 2.2 mol L$^{-1})$ and $(C_o = 2.49 \times 10^{-10}$ and 2.4×10^{-10} mol L$^{-1})$ respectively. The distance between the cited compounds and the ionophore is 2.16 Å indicating the electron transfer mechanism of quenching.

The regression equations were computed and the regression parameters in addition the LOD and LOQ were calculated, and results were presented in Table 1. [LOD $= 3.3S/b$ and LOQ $= 10S/b$, (where S is the standard deviation of blank luminescence intensity values, and b is the slope of the calibration plot)].

3.4.2 Accuracy and precision. The accuracy of the developed method was further investigated *via* applying the standard addition technique and calculating the recovery %. Assessing the obtained recovery was performed through determination of agreement extent between the measured and actual added standard concentration of analyte. All assays were repeated 3 times within the same day and different days to assess the repeatability and intermediate precision, respectively. Three different levels of the analyte concentrations were used in the assays and the results were summarized and presented in (Table 2).

3.4.3 Selectivity. The selectivity of the proposed method was investigated through analyzing placebo blank and synthetically prepared mixtures. All possible interfering inactive compounds were used to prepare a placebo containing; 50 mg calcium carbonate, 20 mg calcium dihydrogen orthophosphate, 30 mg lactose, 100 mg magnesium stearate, 40 methyl cellulose, 70 mg sodium alginate, 300 mg starch and 250 mg Talc. A suitable aliquot of the obtained solution was analyzed after the addition of the optical sensor Tb^{3+}–atorvastatin, and the luminescence spectra were recorded at $\lambda_{ex}/\lambda_{em} = 320/545$ nm following the optimized conditions.

The validity and selectivity were further assessed in presence of some proteins and hormones that may interfere as cortisol, thyroid stimulating hormone, norepinephrine, dopamine, and albumin within concentration range of 0.08 g L^{-1}. The interference of 0.0.06 g L^{-1} urea, 0.08 g L^{-1} glucose, uric acid and folic acid was also studied, and the resulting data revealed that

Table 2 Evaluation of repeatability and intermediate precision of the proposed optical method^a

| Sample	concentration taken ($\times 10^{-7}$ mol L^{-1})	Repeatability			Intermediate precision		
		Average found $\pm$ CL^b	% RE^c	% RSD^d	Drug average found $\pm$ CL	% RE	% RSD
Progesterone in serum	1.0	1.03 ± 0.15	3.00	1.39	1.05 ± 0.21	5.00	3.13
	2.0	1.97 ± 0.14	1.50	1.33	2.04 ± 0.27	2.00	2.12
	4.0	4.07 ± 0.21	1.75	1.99	4.09 ± 0.13	2.25	2.11
Testosterone in serum	1.0	1.04 ± 0.11	4.00	1.46	0.95 ± 0.21	5.00	3.11
	2.0	2.04 ± 0.11	2.00	1.41	2.05 ± 0.26	2.50	2.06
	4.0	3.94 ± 0.16	1.50	1.95	4.08 ± 0.11	2.00	1.02

^{a} $n = 3$. ^{b} CL: confidence limits (ESI). ^{c} % RE: percent relative error (ESI). ^{d} RSD: relative standard deviation.

Table 3 Determination of progesterone and testosterone in serum samples using Tb–Ator optical sensor

Sample	Added ($\times 10^{-7}$ mol L^{-1})	Found ($\times 10^{-7}$ mol L^{-1})	Average[a] ($\times 10^{-7}$ mol L^{-1})	Average recovery $\pm$ % R.S.D	B.P. (LC)
Progesterone serum sample	3.5	3.42, 3.58, 3.60	3.53	100.3 $\pm$ 1.1	98.6 $\pm$ 0.5
	7.0	7.08, 6.95, 7.03	7.02		
	9.5	9.45, 9.56, 9.43	9.48		
Testosterone serum sample	3.5	3.59, 3.43, 3.55	3.52	99.7 $\pm$ 1.5	99.2 $\pm$ 0.6
	7.0	7.05, 6.89, 6.95	6.96		
	9.5	9.61, 9.35, 9.51	9.49		

[a] Average of three measurements.
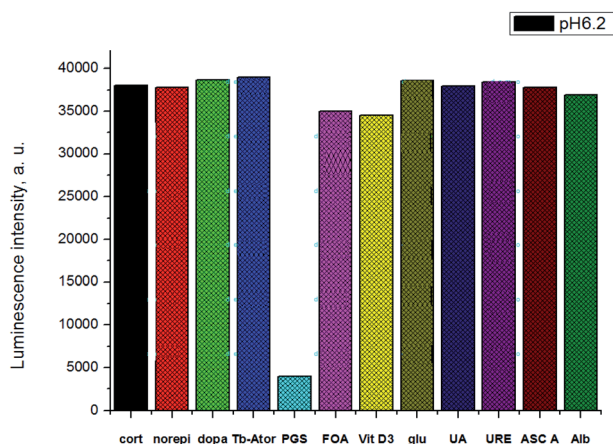
Fig. 12 Effect of interfering species on the luminescence spectrum of Tb–Ator in presence of PGS at pH 6.2.

there was no significant effect on the observed luminescence activity of the proposed photo probe under optimized conditions.

In addition, the proposed optical probe was successfully applied for selective determination of PGS and TST either as single or in combination in synthetically prepared mixtures. Two synthetic mixtures were prepared by adding different concentrations of PGS and TST within their linearity range in 2 similar sets of 10 mL volumetric flasks containing 0.1 mL of the serum sample as mentioned under 2.4.

The pH of the first set was adjusted to 6.2 for selective determination of PGS in presence of TST and the pH of the second set was adjusted to 7.5 for the determination of TST in presence of PGS and the volume was completed with acetonitrile for the two sets. Thus, each mixture was prepared 2 times but at different pH (6.2 and 7.5) for selective estimation of PGS and TST, respectively. Each solution was in triplicates and yielded recovery % of 100.3 $\pm$ 1.10 and 99.6 $\pm$ 1.60 for PGS and TST, respectively.

Therefore, the luminescence of Tb^{3+}–Ator complex with its second coordination sphere in which the dual mixture of PGS and TST is quite sensitive to two variant sets of pHs. For Tb^{3+}–Ator–PGS was of $\lambda_{ex} = 320$ and pH 6.2 and that for Tb^{3+}–Ator–TST was of $\lambda_{ex} = 320$ and pH 7.5. Thus, a dual-controlled luminescence of smoothly dynamic reversibility is achieved and a reversible on/off switchable Tb^{3+} emission of one system was observed by tuning its optimal values of pH to the optimal ones and the second. By this dual controlled luminescence, the dual mixture of PGS and TST was simultaneously resolved with average error < 1.8% in serum sample.

Also, the data obtained upon assaying single PGS and TST separately in serum sample, urine, and dosage form, without any interference from inactive excipients, were processed and results were tabulated as shown in Table 3 and Fig. 12. The results of the proposed method were comparable to that obtained from the reference chromatographic methods mentioned in the British pharmacopeia.[50]

Table 4 Comparison of proposed optical luminescent technique *versus* some previously reported methods for estimation of progesterone and testosterone

Analyte	Methods	Linearity	Limit of detection	References
Progesterone	HPLC-MS-MS	0.2–50 ng mL^{-1}	0.2 ng mL^{-1}	19
	Microfluidic immunosensor system	0.5–12.5 ng mL^{-1}	0.2 ng mL^{-1}	22
	Enzyme-linked fluorescence assay	3–40.0 ng mL^{-1}	—	23
	Spectrofluorometric using Tb^{3+}–Ator	(2.0×10^{-9} to 2.9×10^{-6}) mol L^{-1}	8.5×10^{-10} mol L^{-1}	
Testosterone	HPLC in plasma	1.6–400 ng mL^{-1}	1.6 ng mL^{-1}	32
	HPLC in serum	1–20 ng mL^{-1}	0.4	33
	HPLC in urine	10–500 ng mL^{-1}	1 ng mL^{-1}	33
	HPLC in dosage form	50–200 μg mL^{-1}	5 μg mL^{-1}	31
	HPLC in urine	2–300 ng mL^{-1}	2 ng mL^{-1}	30
	Spectrofluorometric using Tb^{3+}–Ator	(3.1×10^{-9} to 4.8×10^{-6}) mol L^{-1}	7.02×10^{-10} mol L^{-1}	

3.4.4 Comparison with previously reported methods. The results obtained from the proposed spectrofluorometric technique was compared with obtained from other previously reported methods assuring the applicability, accuracy, and precision of the proposed method as presented in Table 4.

4. Conclusion

The proposed analytical method based on the use of Tb^{3+}–atorvastatin complex is simple and economic and can be successfully applied for sensitive and accurate determination of progesterone and testosterone in different matrices including dosage forms, urine, and serum. The analysis of the PGS and TST in biological samples can contribute to early diagnosis of some chronic diseases associated with their abnormal levels.

Conflicts of interest

The authors declare no conflict of interest.

Acknowledgements

References

1 A. L. Attar, M. P. Redekar and N. R. Jadhav, *Curr. Pharm. Res.*, 2016, **6**, 1842–1847.

2 D. Maliwal, P. Jain, A. Jain and V. Patidar, *J. Young Pharma.*, 2009, **1**, 371–374.

3 W. Zhuping, Z. Chao, Y. Chengdui, Z. Xinrong and W. Erruo, *Analyst*, 2000, **125**, 2201–2205.

4 P. Naderi and F. Jalali, *J. Electrochem. Soc.*, 2020, **167**, 027524, DOI: 10.1149/1945-7111/ab6a7f.

5 C. Esmaeili, M. S. Karimi, P. Norouzi, F. Wu, M. R. Ganjali and E. Safitri, *J. Electrochem. Soc.*, 2020, **167**, 067513, DOI: 10.1149/1945-7111/ab828e.

6 A. F. Javier, M. G. Alejandro, M. P. Gabriela, Z. M. Alicia, R. Julio and F. Héctor, *Talanta*, 2010, **80**, 1986–1992.

7 N. Brugger, C. Otzdorff, B. Walter, B. Hoffmann and J. Braun, *Reprod. Domestic Animals*, 2011, **46**, 870–873.

8 C. Yu, Y. Mehrdad, R. H. Barry, P. D. Eleftherios and W. Pui-Yuen, *Clin. Biochem.*, 2009, **42**, 484–490.

9 J. Bain, *Clin. Interv. Aging*, 2007, **2**, 567–576.

10 D. French, *Clin. Chim. Acta*, 2013, **415**, 109–117.

11 R. S. Tan and S. J. Pu, *The Aging Male*, 2003, **6**, 13–17.

12 B. A. Andre, M. D. Julia, A. S. Elizabeth, M. M. Hassan, T. G. Lin and A. W. Gary, *J. Clin. Endocrin. Metab.*, 2011, **96**, 3007–3019.

13 S. P. Tuck and R. M. Francis, *Front. Hormone Res.*, 2009, **37**, 123–132.

14 N. Bassil, S. Alkaade and J. E. Morley, *Therap. Clin. Risk Manag.*, 2009, **5**, 427–448.

15 A. J. Kadhem, S. Xiang, S. Nagel, C.-H. Lin and M. Fidalgo de Cortalezzi, *Polymers*, 2018, **10**, 349–352.

16 M. M. Abd-Elzaher, M. A. Ahmed, A. B. Farag, M. S. Attia, A. O. Youssef and S. M. Sheta, *Sensor Lett*, 2017, **15**, 977–981.

17 L. Konieczna, A. Plenis, I. Olędzka, P. Kowalski and T. Bączek, *Talanta*, 2011, **83**, 804–814.

18 C. He, S. Li, H. Liu, K. Li and F. Liu, *J. Chromatogr., A*, 2005, **1082**, 143–149.

19 R. K. Gupta, R. Roy, A. Chaudhary and A. N. Jha, *Biosci. Biotech. Res. Asia.*, 2010, **7**, 505–511.

20 K. H. Yuen and B. H. Ng, *J. Chromatogr.B.*, 2003, **793**, 421–426.

21 V. Loi, M. Vertzoni, A. Vryonidou and C. Phenekos, *J.Pharma. Biomed. Anal.*, 2006, **41**, 527–532.

22 J. Albrethsen, M. L. Ljubicic and A. Juul, *J. Clin. Endocrin. Metabol.*, 2020, **105**(10), dgaa496.

23 S. Alvi and M. Hammami, *J. Advanced Pharma. Techn. Res.*, 2020, **11**, 64, DOI: 10.4103/japtr.japtr_162_19.

24 W. C. Chang, D. A. Cowan, C. J. Walker, N. Wojek and A. D. Brailsford, *J. Chroma. A*, 2020, **1628**, 461445, DOI: 10.1016/j.chroma.2020.461445.

25 X. Li, T. Yuan, T. Zhao, X. Wu and Y. Yang, *J. Chroma. Sci.*, 2020, **58**(9), 880–886, DOI: 10.1093/chromsci/bmaa051.

26 W. Xu, H. Li, Q. Guan, Y. Shen and L. Cheng, *JCLA J. Clinic. Lab. Anal.*, 2017, **31**, e22102, DOI: 10.1002/jcla.22102.

27 R. Heidarimoghadam, O. Akhavan, E. Ghaderibi, E. Hashemi, S. S. Mortazavi and A. Farmany, *Materials Sci. Eng: C.*, 2016, **61**, 246–250.

28 K. H. Liu, D. O'Hare, J. L. Thomas, H. Z. Guo, C. H. Yang and M. H. Lee, *Biosensors*, 2020, **10**, 16, DOI: 10.3390/bios10030016.

29 B. Du, J. Zhang, Y. Dong, J. Wang, L. Lei and R. Shi, *Steroids*, 2020, **161**, 108691, DOI: 10.1016/j.steroids.2020.108691.

30 U. Turpeinen, S. Linko, O. Itkonen, E. Hämäläinen and E. Scandinavian, *J. Clin. Lab. Invest.*, 2008, **68**, 50–57.

31 M. S. Attia, W. H. Mahmoud, A. O. Youssef and M. S. Mostafa, Cilostazol Determination by the Enhancement of the Green Emission of Tb^{3+} Optical Sensor, *J. Fluoresc.*, 2011, **21**, 2229–2235, DOI: 10.1007/s10895-011-0927-y.

32 M. S. Attia, M. H. Khalil, M. S. A. Abdel-Mottaleb, M. B. Lukyanova, Yu. A. Alekseenko and B. Lukyanov, Effect of Complexation with Lanthanide Metal Ions on the Photochromism of (1, 3, 3-Trimethyl-5_-Hydroxy-6_-Formyl-Indoline-Spiro2, 2-[2H] chromene) in Different Media, *Int. J. Photoenergy*, 2006, 1–9, DOI: 10.1155/ijp/2006/42846.

33 M. S. Attia, A. A. Essawy, A. O. Youssef and M. S. Mostafa, Determination of Ofloxacin using a Highly Selective Photo Probe Based on the Enhancement of the Luminescence Intensity of Eu^{3+} - Ofloxacin Complex in Pharmaceutical and Serum Samples, *J. Fluoresc.*, 2012, **2**, 557–564, DOI: 10.1007/s10895-011-0989-x.

34 M. S. Attia, A. M. Othman, A. O. Youssef and E. El-Raghi, Excited state interaction between Hydrochlorothiazide and Europium ion in PMMA polyme, and its application as optical sensor for Hydrochlorothiazide in tablet and serum samples, *J. Lumines.*, 2012, **132**, 2049–2053, DOI: 10.1016/j.jlumin.2012.03.012.

35 M. S. Attia, A. O. Youssef and A. A. Essawy, A novel method for tyrosine assessment in vitro by using fluorescence enhancement of the ion-pair tyrosine- neutral red dye photo probe, *Anal. Methods*, 2012, **4**, 2323–2328, DOI: 10.1039/c2ay25089f.

36 M. S. Attia, A. O. Youssef and R. H. El-Sherif, Durable diagnosis of seminal vesicle and sexual gland diseases using the nano optical sensor thin film sm-doxycycline complex, *Anal. Chim. Acta*, 2014, **835**, 56–64, DOI: 10.1016/j.aca.2014.05.016.

37 M. S. Attia, M. Diab and M. F. El-Shahat, Diagnosis of some diseases related to the histidine level in human serum by using the nano optical sensor Eu–Norfloxacine complex, *Sensors and Actuators B*, 2015, **207**, 756–763, DOI: 10.1016/j.snb.2014.10.132.

38 M. S. Attia, A. O. Youssef, Z. A. Khan and M. N. Abou-Omar, Alpha fetoprotein assessment by using a nano optical sensor thin film binuclear Pt-2-aminobenzimidazole-Bipyridine for early diagnosis of liver cancer, *Talanta*, 2018, **186**, 36–43, DOI: 10.1016/j.talanta.2018.04.043.

39 M. S. Attia and N. S. Al-Radadi, Progress of pancreatitis disease biomarker alpha amylase enzyme by new nano optical sensor, *Biosens. Bioelect.*, 2016, **86**, 413–419, DOI: 10.1016/j.bios.2016.06.079.

40 M. S. Attia and N. S. Al-Radadi, Nano optical sensor binuclear Pt-2-pyrazinecarboxylic acid-bipyridine for enhancement of the efficiency of 3-nitrotyrosine biomarker for early diagnosis of liver cirrhosis with minimal hepatic encephalopathy, *Biosens. Bioelect.*, 2016, **86**, 406–412, DOI: 10.1016/j.bios.2016.06.074.

41 M. S. Attia, Nano optical probe samarium tetracycline complex for early diagnosis of histidinemia in newborn children, *Biosens. Bioelect.*, 2017, **94**, 81–86, DOI: 10.1016/j.bios.2017.02.018.

42 M. S. Attia, K. Ali, M. El-Kemary and W. M. Darwish, Phthalocyanine-doped polystyrene fluorescent nanocomposite as a highly selective biosensor for quantitative determination of cancer antigen 125, *Talanta*, 2019, **201**, 185–193, DOI: 10.1016/j.talanta.2019.03.119.

43 M. S. Attia, M. N. Ramsis, L. H. Khalil and S. G. Hashem, Spectrofluorimetric assessment of chlorzoxazone and Ibuprofen in pharmaceutical formulations by using Eu-tetracycline HCl optical sensor doped in sol–gel matrix, *J. Fluoresc.*, 2012, **22**, 779–788, DOI: 10.1007/s10895-011-1013-1.

44 A. A. Elabd and M. S. Attia, A new thin film optical sensor for assessment of UO22+ based on the fluorescence quenching of Trimetazidine doped in sol gel matrix, *J. Lumines.*, 2015, **165**, 179–184, DOI: 10.1016/j.jlumin.2015.04.024.

45 A. A. Elabd and M. S. Attia, Spectroflourimetric assessment of UO22+ by the quenching of the fluorescence intensity of Clopidogrel embedded in PMMA matrix, *J. Lumines.*, 2016, **169**, 313–318, DOI: 10.1016/j.jlumin.2015.04.024.

46 A. A. Essawy and M. S. Attia, Novel application of pyronin Y fluorophore as high sensitive optical sensor of glucose in human serum, *Talanta*, 2013, **107**, 18–24, DOI: 10.1016/j.talanta.2012.12.033.

47 E. Hamed, M. S. Attia and K. Bassiony, Synthesis, spectroscopic and thermal characterization of Copper (II) complexes of folic acid and their absorption efficiency in the blood, *J. Bioinorg. chem. appl.*, 2009, 1–7, DOI: 10.1155/2009/979680.

48 M. S. Attia, K. Ali, M. El- Kemary and W. M. Darwish, Phthalocyanine-doped polystyrene fluorescent nanocomposite as a highly selective biosensor for quantitative determination of cancer antigen 125, *Talanta*, 2019, **201**, 185–193.

49 I. H. T. Guideline, Validation of analytical procedures: text and methodology. Q2 (R1), **1**, 1–15, 2005.

50 Stationery Office (Great Britain), *British pharmacopoeia 2009*, Stationery Office, London, 2008.